Am J Physiol Heart Circ Physiol 292: H2952–H2958, 2007.
First published February 16, 2007; doi:10.1152/ajpheart.01356.2006.

Absence of diastolic mitral annular oscillations is a marker for relaxation-related diastolic dysfunction

Matt M. Riordan[2] and Sándor J. Kovács[1,2]

Cardiovascular Biophysics Laboratory, Cardiovascular Division, [1]Department of Internal Medicine, Washington University School of Medicine and [2]Department of Biomedical Engineering, School of Engineering and Applied Science, Washington University, St. Louis, Missouri

Submitted 12 December 2006; accepted in final form 9 February 2007

Riordan MM, Kovács SJ. Absence of diastolic mitral annular oscillations is a marker for relaxation-related diastolic dysfunction. *Am J Physiol Heart Circ Physiol* 292: H2952–H2958, 2007. First published February 16, 2007; doi:10.1152/ajpheart.01356.2006.—Although Doppler tissue imaging frequently indicates the presence of mitral annular oscillations (MAO) following the E′ wave (E″ wave, etc.), only recently was it shown that annular "ringing" follows the rules of damped harmonic oscillatory motion. Oscillatory model-based analysis of E′ and E″ waves provides longitudinal left ventricular (LV) stiffness (k'), relaxation/viscoelasticity (c'), and stored elastic strain (x_o') parameters. We tested the hypothesis that presence (MAO^+) vs. absence (MAO^-) of diastolic MAO is an index of superior LV relaxation by analyzing simultaneous echocardiographic-hemodynamic data from 35 MAO^+ and 20 MAO^- normal ejection fraction (EF) subjects undergoing cardiac catheterization. Echocardiographic annular motion and transmitral flow data were analyzed with a previously validated kinematic model of filling. Invasive and noninvasive diastolic function (DF) indexes differentiated between MAO^+ and MAO^- groups. Specifically, the MAO^+ group had a shorter time constant of isovolumic relaxation [τ; 51 (SD 13) vs. 67 (SD 27) ms; $P < 0.01$] and isovolumic relaxation time [63 (SD 16) vs. 82 (SD 17) ms; $P < 0.001$] and greater ratio of peak E-wave to peak A-wave velocity [1.19 (SD 0.31) vs. 0.97 (SD 0.31); $P < 0.05$]. The MAO^+ group had greater peak lateral mitral annulus velocity [E′; 17.5 (SD 3.1) vs. 13.5 (SD 3.8) cm/s; $P < 0.001$] and LVEF [71.2 (SD 7.5)% vs. 65.4 (SD 9.1)%; $P < 0.05$] and lower heart rate [65 (SD 9) vs. 74 (SD 9) beats/min, $P < 0.001$]. Additional conventional and kinematic modeling-derived indexes were highly concordant with these findings. We conclude that absence of early diastolic MAO is an easily discernible marker for relaxation-related diastolic dysfunction. Quantitation of MAO via stiffness and relaxation/viscoelasticity parameters facilitates quantitative assessment of regional (i.e., longitudinal) DF and may improve diagnosis of diastolic dysfunction.

E′ wave; mitral annular motion; echocardiography; mathematical modeling; diastolic function; Doppler tissue imaging

HEART FAILURE with a normal left ventricular (LV) ejection fraction (EF), or "diastolic heart failure," is a growing epidemic (34). Diastolic dysfunction (DD) itself has substantial adverse prognostic significance, demonstrating the importance of proper diagnosis of DD (35). While invasive diastolic function (DF) characterization typically involves the measurement of LV pressure and volume via cardiac catheterization, noninvasive DF characterization is usually achieved with echocardiography (2). Although new techniques for DF assessment, including strain, strain-rate, and color Doppler M mode, are evolving (30), evaluation of the transmitral flow pattern in concert with Doppler tissue imaging (DTI) remains a common method for DF assessment (2). Certain geometric features of the E and A waves, usually approximated as triangles, have been correlated with dysfunction [i.e., ratio of peak E-wave to peak A-wave velocity (E/A), deceleration time (DT), acceleration time (AT), velocity-time integral (VTI), etc.]. However, the known load dependence of global indexes, the realization that they may not be as sensitive to subtle mechanical dysfunction as regional indexes, and the evolution of imaging technology (strain, strain-rate, color Doppler M-mode, etc.) have led to increased interest in segmental or regional DF characterization. In particular, recent DTI studies have found that the long-axis (longitudinal) motion of the LV during early filling is much less load dependent than the E wave (13, 29, 30). This finding has motivated more routine measurement of the peak E′-wave velocity (E′) as an index of longitudinal DF. However, similar to E and A wave-based indexes, longitudinal DTI-based indexes currently rely only on geometric features (i.e., peaks) of the annular velocity contour, approximated as a triangle, and do not utilize the information content of the curvilinear velocity contour. Furthermore, E/E′, commonly reported as a noninvasive correlate of LV filling pressure, is computed from the nonsimultaneous peak values of the E and E′ waves (26).

MODELING LONGITUDINAL DIASTOLIC FUNCTION

To more completely characterize longitudinal DF in terms of stiffness and relaxation/viscoelasticity, we previously applied and validated damped simple harmonic oscillatory (SHO) motion as the kinematic principle that governs mitral annular oscillations (MAO) (38). Because LV filling is initiated by mechanical suction (defined as a simultaneous decrease in pressure and increase in volume, i.e., $dP/dV < 0$ immediately after mitral valve opening), a component of which must manifest as longitudinal elastic recoil, the proposed kinematic model for annular motion complements a previously developed and validated global lumped-parameter model that accurately predicts transmitral flow patterns (21, 24). This global model has validated relaxation during early filling as an important indicator of disease (9, 22, 37) and elucidated its relationship to isovolumic relaxation time (IVRT) and the time constant of isovolumic relaxation (τ) (8).

Accordingly, longitudinal tissue motion at the annulus (i.e., the E′ wave) can be characterized to excellent approximation

Address for reprint requests and other correspondence: S. J. Kovács, Cardiovascular Biophysics Laboratory, Washington Univ. Medical Center, Box 8086, 660 South Euclid Ave., St. Louis, MO 63110 (e-mail: sjk@wuphys.wustl.edu).

The costs of publication of this article were defrayed in part by the payment of page charges. The article must therefore be hereby marked "*advertisement*" in accordance with 18 U.S.C. Section 1734 solely to indicate this fact.

in analogy to the motion of a previously displaced (stretched) oscillator recoiling from rest by considering the balance of inertial, elastic, and viscous forces during early filling (38). This paradigm, the parameterized diastolic filling (PDF) formalism, has been successfully applied to E-wave analysis and can be similarly applied to annular motion. It provides longitudinal indexes of DF by using the clinical E′-wave contour as input and generating unique values for the initial spring displacement (x'_o), damping constant (c'), and spring constant (k') of an equivalent SHO. The physiological analogs of x'_o, c', and k' are the VTI of the E′ wave, longitudinal myocardial relaxation/viscoelasticity, and longitudinal myocardial stiffness, respectively. Importantly, besides its observer-independent aspects, a key advantage of the PDF formalism is that it is "predictive" rather than "accommodative" in characterizing the E′-wave contour (25).

Interestingly, in addition to permitting solution to the "inverse problem" of longitudinal DF (38), the paradigm of a damped SHO for the E′ wave naturally predicts, and easily accounts for, the frequently observed reversal in the direction of motion (i.e., "ringing") of the annulus. This oscillatory motion can be described by the mass-normalized solution to the equation of motion for a SHO:

$$v(t) = -\frac{k' x'_o}{\omega'} e^{-\alpha' t} \sin(\omega' t) \qquad (1)$$

where $\alpha' = c'/2$, $\omega' = [(4 \cdot k' - c'^2)^{1/2}]/2$. For underdamped oscillation, where relaxation/viscoelastic effects are dominated by stiffness (i.e., $c'^2 < 4 \cdot k'$), a MAO (described by the E″ wave) is predicted. Conversely, for overdamped or critically damped motion, in which relaxation/viscoelastic effects dominate stiffness (i.e., $c'^2 \geq 4 \cdot k'$), the model predicts absence of mitral annular oscillations (MAO^-). Therefore, the physics governing annular kinematics naturally dichotomizes subjects into those with and those without annular oscillations based on the relative values of c' and k'. Furthermore, this kinematic analysis must be obeyed physiologically in the sense that a given LV either will or will not exhibit MAO.

The presence of MAO (i.e., the E″ wave) has been previously observed in humans (19, 42), but elucidation and characterization beyond noting mere presence have been lacking. Accordingly, we sought to test the hypothesis that if subjects were grouped according to the kinematically mandated presence (MAO^+) or absence (MAO^-) of annular oscillations, the dichotomization would elucidate DF differences between the groups. Specifically, we hypothesized that the absence of annular oscillations (MAO^-) is the consequence of greater longitudinal relaxation/viscoelasticity effects relative to longitudinal stiffness and, therefore, implies worse DF than the presence of annular oscillations (MAO^+).

METHODS

Patient selection. A sample of 55 normal LVEF (i.e., >50%) subjects with high-quality contemporaneous echocardiographic recordings of transmitral Doppler flow and DTI recordings of the lateral mitral annulus and high-fidelity (Millar) LV pressure were obtained from an existing database (8, 27). All subjects gave informed consent in accordance with a protocol approved by the Washington University Medical Center Human Studies Committee (Institutional Review Board) before data acquisition and catheterization. Before data acquisition and catheterization, all subjects gave informed consent according to Washington University Medical Center Human Studies (Institutional Review Board) guidelines. Subjects with abnormalities that could affect MAO, such as mitral stenosis, calcification, or regurgitation, were excluded. Subjects with heart rate (HR) sufficiently high to cause merging of the E′ and A′ waves (precluding identification of MAO) were also excluded. The subjects, ranging in age from 32 to 72 yr [54.5 (SD 9.9) yr], were dichotomized according to the presence (MAO^+, $n = 35$) or absence (MAO^-, $n = 20$) of MAO (i.e., the E″ wave). If a subject exhibited clear annular oscillations on at least three beats, he/she was entered into the MAO^+ group. If a subject had no annular oscillations on any recorded beat, he/she was entered into the MAO^- group. Subjects with one or two oscillatory beats were not included in the study. In general, annular oscillations were highly reproducible from beat to beat in the MAO^+ group. The groups did not differ with respect to age, height, weight, race, or gender, and the number of subjects on diuretics, beta blockers, alpha blockers, angiotensin-converting enzyme inhibitors, and nitrates also did not differ between groups. Both groups included subjects with various nonvalvular comorbidities including, but not limited to, hypertension, diabetes, angiographically diagnosed coronary artery disease (CAD), previous myocardial infarction, wall motion abnormalities on ventriculography, cardiomyopathy, and a history of transient renal dysfunction. Hypertension, diabetes, and CAD were the most common comorbidities and, like the others, were comparably present in each group. Importantly, none of the subjects in either group had active ischemia at the time of data acquisition. A total of 20 subjects had elevated filling pressures defined as LV end-diastolic pressure (LVEDP) > 18 mmHg, and 28 subjects had impaired relaxation defined as $\tau > 50$ ms. Five MAO^+ and seven MAO^- subjects had elevated τ in addition to elevated LVEDP based on these criteria. Notably, diagnosis of DD does not require simultaneous presence of both elevated LVEDP and prolonged τ. In contrast, subjects without clinical evidence of advanced DD may exhibit impaired stiffness or relaxation in isolation (12). However, we note that in general, subjects with elevated filling pressures tend to have impaired relaxation, although the inverse is often not true. Table 1 displays the relevant demographic and clinical information for each group.

Elective cardiac catheterization was performed on all subjects at the request of their referring physician on the basis of suspected CAD. Since the primary aim of this study was to determine the stiffness, relaxation/viscoelasticity, and stored elastic strain-based physiological mechanisms that cause (or prevent) oscillations of the mitral annulus in any heart, we specifically chose not to compare healthy

Table 1. *Subject variables*

Attribute	MAO^+ Group ($n = 35$)	MAO^- Group ($n = 20$)	Intergroup Significance
Age, yr	53 (10)	56 (10)	P = NS
Males	25	12	P = NS
Minorities	5	6	P = NS
LVEDP > 18 mmHg and $\tau < 50$ ms	7	0	$P < 0.05$
LVEDP ≤ 18 mmHg and $\tau > 50$ ms	9	7	P = NS
Hypertensive	10	2	P = NS
Diabetic	6	1	P = NS
CAD	9	5	P = NS
Height, cm	175 (10)	173 (12)	P = NS
Weight, kg	93 (23)	92 (14)	P = NS
HR, beats/min	65 (9)	74 (9)	$P < 0.001$

Clinical parameter values are means (SD), and demographic values are numbers of subjects. MAO^+, subjects with mitral annular oscillations; MAO^-, subjects without mitral annular oscillations; CAD, coronary artery disease; HR, heart rate; LVEDP, left ventricular end-diastolic pressure; τ, time constant of isovolumic relaxation; NS, not significant.

controls vs. a single pathological group (hypertension, diabetes, CAD, heart failure, etc.). Hence, the MAO$^-$ group had multiple clinical comorbidities, as expected.

Data acquisition. The methodology has been previously described (8, 27). Briefly, immediately before cardiac catheterization, a full two-dimensional/Doppler examination was performed in the catheterization laboratory with a standard clinical imaging system (Acuson, Mountain View, CA) including DTI of the lateral mitral annulus and transmitral Doppler inflow according to American Society of Echocardiography criteria (15). DTI for 11 of the subjects was performed with somewhat larger sample volumes (5, 9, and 10 mm). Previous DTI studies have used sample volumes ranging from 2 to 10 mm (14, 28–30, 39). All images were captured and stored on magneto-optical disks. A micromanometric 6-Fr, dual-pressure transducer pigtail catheter (model SPC-560, Millar Instruments, Houston, TX) was advanced into the LV through a 6-F sheath (Arrow, Reading, PA) in the femoral artery. Pressure was recorded via a custom data acquisition system.

Doppler analysis. For each subject, five diastolic intervals containing clear E and A waves were selected and converted to 8-bit grayscale images with Paint Shop Pro 7 (Jasc Software, Minnetonka, MN). Conventional echocardiographic parameters AT, DT, peak E- and A-wave velocity, and E- and A-wave VTI (VTI_E and VTI_A, respectively) were measured manually with the triangle approximation for wave shape and averaged. IVRT was measured as the time between closure of the aortic valve and opening of the mitral valve (15). E-wave analysis using the PDF formalism was performed via model-based image processing according to previously validated methods to output the (mathematically) unique best-fit kinematic parameters (16, 17, 21). The parameters c (g/s) and k (g/s^2) denote the SHO (global) damping constant and spring constant (i.e., stiffness, dP/dV; Ref. 27), respectively. The parameter x_o (cm) corresponds to the stored elastic strain available at mitral valve opening that facilitates mechanical recoil (21, 23). All parameters are computed per unit mass (m). Additional SHO-derived indexes include kx_o, the peak force (equivalent to the peak atrioventricular pressure gradient) (4), $1/2kx_o^2$, the stored elastic strain energy associated with LV recoil during filling, and β, a viscoelastic stiffness parameter that quantitates the relative contributions of stiffness (k) and relaxation/viscoelasticity (c) in determining the E-wave contour ($\beta = c^2 - 4mk$).

Three to five DTI cardiac cycles from each subject containing E′ and A′ waves were also selected, clipped, and converted to grayscale images. Peak E′- and A′-wave velocities were determined, as well as E′- and A′-wave VTIs ($VTI_{E'}$ and $VTI_{A'}$, respectively), by triangle approximation. For subjects with annular oscillations (i.e., an E″ wave), peak E″-wave velocity (E″) and E″-wave VTI ($VTI_{E''}$) were also determined. Lateral mitral annular excursion during early filling was determined by subtracting $VTI_{E''}$ from $VTI_{E'}$ for subjects in the MAO$^+$ group. E′-wave analysis was performed analogously to E-wave analysis via model-based image processing and nonlinear least-squares fitting of the model-predicted annular velocity (*Eq. 1*) to the actual mitral annulus velocity contour as previously detailed (38). The longitudinal parameters c' (g/s) and k' (g/s^2) denote the longitudinal damping constant and spring constant of the system, respectively, determined from the E′ wave. Additional longitudinal indexes include $k'x'_o$, the peak longitudinal force driving recoil, $1/2k'x'^2_o$, the peak stored elastic strain energy, and β', where $\beta' = c'^2 - 4mk'$ (38). Figure 1 shows an example of the SHO model fit to an oscillatory and a nonoscillatory beat from representative subjects in the MAO$^+$ and MAO$^-$ groups, respectively.

For the MAO$^+$ group, longitudinal c' was determined by fitting a decaying exponential from the peak of the E′ wave to the peak of the E″ wave, as previously described (38). For the MAO$^-$ group, longitudinal c' was determined by assuming critical damping, which has slight limitations, as previously discussed (38).

Hemodynamic analysis. LVEDP, minimum LV pressure (LVP_{min}), and LV pressure at diastasis (LVP_{diast}) were determined from the LV pressure tracing, and the time constant of isovolumic relaxation τ was computed from the LV pressure "phase plane" (11) [i.e., the plot of the 1st derivative of pressure (dP/dt) vs. pressure (P)], which allows for nonzero pressure asymptotes, for five consecutive beats. The slope of the linear best fit from just after dP/dt_{min} to just before mitral valve opening defines $-1/\tau$ (8). LV end-systolic volume (LVESV) was determined from suitably calibrated ventriculography. These and related hemodynamic indexes are listed in Table 2.

Statistical analysis. All data are displayed as means (SD). Statistical differences between the subjects with and without MAO were determined by two-tailed analysis of variance. Statistical analysis of the nominal data for gender and minority representation, representative comorbidities, DD based on cutoff values for LVEDP and τ (see Table 1), and pertinent medications in each group was performed with the two-tailed z-test for proportions. All statistical calculations were performed in Microsoft Excel 97 (Microsoft, Redmond, WA). Statistical significance was at the $P < 0.05$ level.

RESULTS

The values of all DTI measurements, parameters, and indexes analyzed for both groups are displayed in Table 3. Conventional Doppler and hemodynamic measurements, parameters, and indexes are shown in Table 2.

Major findings. Group comparison showed that the MAO$^+$ group had a shorter τ ($P < 0.01$) and IVRT ($P < 0.001$) and greater E/A ($P < 0.05$), indicating prolonged relaxation in subjects with MAO$^-$. The MAO$^+$ group also had greater E′ ($P < 0.0001$), slightly greater EF ($P < 0.05$), and lower HR ($P < 0.001$). The quantity $LVP_{diast} - LVP_{min}$ was also greater in the MAO$^+$ group.

Additional concordant findings. Additional conventional and kinematic parameters/indexes of global and longitudinal LV function corroborate these findings. Specifically, among the

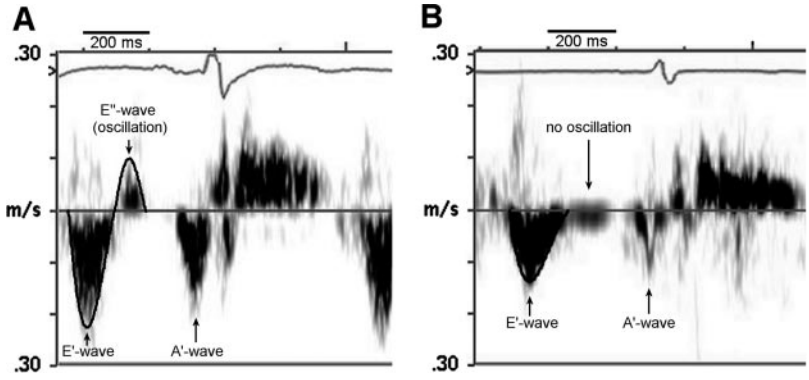

Fig. 1. *A*: representative Doppler tissue imaging (DTI) images of the mitral annulus from a subject having mitral annular oscillations (MAO) on each beat. The model-predicted fit (solid black line) is superimposed on the raw DTI image. Note the E″ wave (oscillation) following the E′ wave. Each (E′, E″) wave is very closely fit by the model. Best-fit parameters for the E′ wave are $c' = 14.5$ g/s, $k' = 561$ g/s^2, $x'_o = 1.3$ cm. *B*: representative DTI annular motion image from a subject having no MAO on any beat examined. The model-predicted fit (solid black line) is superimposed on the raw DTI image. The E′ wave is very closely fit by the model, yielding best-fit parameters of $c' = 19.2$ g/s, $k' = 371$ g/s^2, and $x'_o = 1.3$ cm. Note the lower peak E′-wave velocity and more elongated deceleration portion of the E′ wave compared with A.

Table 2. *Conventional and PDF parameters/indexes*

Parameter/Index	MAO$^+$ Group (n = 35)	MAO$^-$ Group (n = 20)	Intergroup Significance
EF, %	71.2 (7.5)	65.4 (9.1)	***P* < 0.05**
E, cm/s	70.2 (15.0)	66.0 (15.5)	$P = 0.34$
AT, ms	87 (13)	92 (13)	$P = 0.13$
DT, ms	184 (40)	205 (53)	$P = 0.11$
VTI_E, mm	95 (20)	100 (26)	$P = 0.47$
A, cm/s*	61.5 (13.6)	74.1 (21.2)	***P* < 0.05**
VTI_A, mm*	47 (10)	51 (17)	$P = 0.37$
E/A*	1.19 (0.31)	0.97 (0.31)	***P* < 0.05**
IVRT, ms	63 (16)	82 (17)	***P* < 0.001**
τ, ms†	51 (13)	67 (27)	***P* < 0.01**
LVESV, ml†	48 (24)	61 (29)	$P = 0.08$
LVEDP, mmHg	16.8 (4.5)	17.9 (5.4)	$P = 0.44$
LVP_{min}, mmHg†	6.3 (3.5)	7.0 (4.3)	$P = 0.54$
LVP_{diast}, mmHg†	11.0 (4.5)	10.5 (4.1)	$P = 0.69$
$LVP_{diast} - LVP_{min}$, mmHg†	4.7 (1.6)	3.6 (1.2)	***P* < 0.05**
dP/dt_{min}, mmHg/s†	−1,731 (263)	−1,636 (414)	$P = 0.30$
c, g/s	18.4 (5.9)	27.3 (10.4)	***P* < 0.001**
k, g/s^2	204 (38)	225 (69)	$P = 0.15$
x_o, cm	10.5 (2.9)	11.7 (3.4)	$P = 0.17$
kx_o, dyn	2,100 (660)	2,590 (1,000)	***P* < 0.05**
$1/2kx_o^2$, erg	11,700 (7,100)	16,100 (10,300)	$P = 0.07$
β, s^{-2}	−445 (254)	−54 (542)	***P* < 0.001**

Values are means (SD). EF, ejection fraction; E and A, peak amplitude of E and A wave, respectively; AT and DT, acceleration and deceleration time of E wave, respectively; VTI_E and VTI_A, velocity-time integral of E and A wave, respectively; IVRT, isovolumic relaxation time; τ, time constant of isovolumic relaxation; LVESV, left ventricular (LV) end-systolic volume; LVEDP, LV end-diastolic pressure; LVP_{min}, minimum LV pressure; LVP_{diast}, diastolic LV pressure; dP/dt_{min}, peak negative rate of pressure decline during isovolumic relaxation; c, damping constant; k, spring constant; x_o, initial displacement of spring before release; β, effect of stiffness vs. relaxation. *E and A waves were merged in 3 of the subjects without annular oscillations, precluding determination of A, E/A, and VTI_A for these subjects. †Technical difficulties during data acquisition precluded determination of LVESV, LVP_{min}, LVP_{diast}, and $LVP_{diast} - LVP_{min}$ in 1 and τ and dP/dt_{min} in 2 of the subjects without annular oscillations, respectively. Bold type indicates significance.

conventional indexes, the MAO$^+$ group had greater E′/A′ ($P < 0.05$) and $VTI_{E'}$ ($P < 0.0001$), greater annular excursion ($VTI_{E'} - VTI_{E''}$) ($P < 0.05$), and lower E/E′ ($P < 0.05$) and A ($P < 0.05$). In longitudinal PDF parameter/index terms (see Table 3), the MAO$^+$ group had lower c' ($P < 0.00001$) and k' ($P < 0.05$), greater x'_o ($P < 0.01$), $k'x'_o$ ($P < 0.05$), and $\frac{1}{2}k'x'^2_o$ ($P < 0.01$), and more negative β' ($P < 0.00001$). In global PDF parameter/index terms (see Table 2), the MAO$^+$ group had lower c ($P < 0.001$), lower kx_o ($P < 0.05$), and more negative β ($P < 0.001$).

Intraobserver variation for both global and longitudinal PDF parameters has been previously assessed. The coefficients of variation (5) for c, k, and x_o were determined to be 2.8%, 1.2%, and 3.6%, respectively (37). The coefficients of variation for c', k', and x'_o were determined to be 2.5%, 5.1%, and 6.5%, respectively (38).

Absence of MAO had a sensitivity of 62.2% and a specificity of 74.2% for identifying impaired relaxation-related DF according to $\tau > 50$ ms. Figure 2 illustrates the predictive ability of MAO$^-$, as well as some conventional noninvasive relaxation indexes, for $\tau > 50$ ms via receiver-operator characteristic curves, which were constructed by previously established methods (18). The selected cutoff values for IVRT and DT, as well as τ, are based on values commonly cited in the literature (10, 12, 13).

Age dependence of MAO. Since the MAO$^+$ group had better DF than the MAO$^-$ group based on a variety of invasive and noninvasive indexes (including τ, IVRT, E/A, and E′/A′) and DF indexes are known to depend on age (32, 33, 36), we also investigated the age dependence of MAO$^+$. Figure 3 displays the percentage of subjects as a function of age expressed in decade intervals. The bar chart shows that the percentage of MAO$^+$ subjects decreases monotonically with age, implying that presence or absence of MAO, in concordance with the aforementioned Doppler indexes, depends on age.

DISCUSSION

Cardiac anatomy and physiology. Zaky et al. (42) were the first to note that motion of the mitral annulus may have clinical importance. They noted that annular motion often reverses direction after the initial E′ wave. Much later, Isaaz et al. (19) described the continuous, alternating atrially and apically directed motion of the mitral annulus during the cardiac cycle and hypothesized that the balance between stored elastic potential energy and kinetic energy plays a role. Recently, we complemented and extended these descriptive approaches, as well as others (19, 20, 40–42), by introducing and validating a quantitative, kinematics-based method of longitudinal DF assessment (38). This method views longitudinal annular motion during early filling as driven by strain energy (titin, extracellular matrix, etc.) stored during the previous systole; because of inertial effects and depending on the relative magnitudes of stiffness and viscoelasticity, the annulus "overshoots" its equilibrium position and reverses direction (toward the apex) in certain subjects. The physics governing oscillatory motion predicts an oscillatory (stiffness > viscoelasticity) regime for annular motion as well as a nonoscillatory (stiffness < viscoelasticity) regime. Both regimes are observed

Table 3. *Conventional and PDF parameters/indexes of longitudinal diastolic function*

Parameter/Index	MAO$^+$ Group (n = 35)	MAO$^-$ Group (n = 20)	Intergroup Significance
E′, cm/s	17.5 (3.1)	13.5 (3.9)	***P* < 0.00001**
AT′, ms	65 (12)	54 (11)	***P* < 0.01**
DT′, ms	79 (17)	67 (20)	***P* < 0.05**
$VTI_{E'}$, mm	12.7 (3.5)	8.3 (3.7)	***P* < 0.0001**
$VTI_{E'} - VTI_{E''}$, mm*	10.4 (3.6)	8.3 (3.7)	***P* < 0.05**
A′, cm/s	16.3 (3.6)	15.5 (3.5)	$P = 0.42$
$VTI_{A'}$, mm	7.3 (2.3)	8.6 (3.0)	$P = 0.06$
E′/A′	1.11 (0.28)	0.91 (0.35)	***P* < 0.05**
E/E′	4.16 (1.15)	5.18 (1.80)	***P* < 0.05**
c', g/s	18.3 (5.9)	48.6 (7.7)	***P* < 0.00001**
k', g/s^1	490 (120)	594 (233)	***P* < 0.05**
x'_o, cm	1.16 (0.32)	0.85 (0.45)	***P* < 0.01**
$k'x'_o$, dyn	547 (153)	460 (149)	***P* < 0.05**
$\frac{1}{2}k'x'^2_o$, erg	337 (164)	217 (147)	***P* < 0.01**
β', s^{-2}†	−1,787 (489)	0 (0)	***P* < 0.00001**

Values are means (SD). E′ and A′, peak amplitude of E′ and A′ wave, respectively; AT′ and DT′, acceleration and deceleration time of E′ wave, respectively; $VTI_{E'}$ and $VTI_{E''}$, velocity-time integral of E′ and E″ wave, respectively; $VTI_{A'}$, velocity-time integral of A′ wave; E, peak amplitude of E wave; c', longitudinal damping constant; k', longitudinal spring constant; (x'_o), initial longitudinal displacement of spring before release; β', effect of longitudinal stiffness vs. relaxation. *E″ waves were absent in subjects without annular oscillations. †β' was computed for the MAO$^-$ subjects by assuming critical damping as discussed in METHODS. Bold type indicates significance.

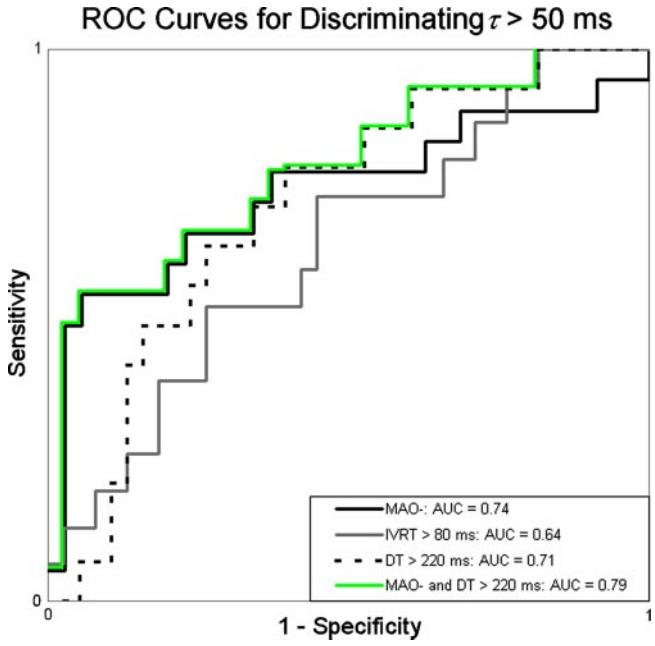

Fig. 2. Receiver-operator characteristic curves for absence of MAO (MAO^-), isovolumic relaxation time (IVRT) > 80 ms, deceleration time (DT) > 220 ms, and MAO^- and DT > 220 ms (in combination) for predicting time constant of isovolumic relaxation (τ) > 50 ms (relaxation-related diastolic dysfunction). Note that the area under the MAO^- curve (AUC) is the greatest for all curves determined from a single marker, implying that absence of MAO is more predictive of $\tau > 50$ ms than either IVRT > 80 ms or DT > 220 ms. The associated sensitivity and specificity of MAO^- for $\tau > 50$ ms are 62.2% and 74.2%, respectively. However, when the MAO^- and DT > 220 ms markers are used in tandem, the AUC increases by 5%.

physiologically via DTI, and, as predicted, relaxation/viscoelasticity dominates stiffness in MAO^- subjects. Hence, the paradigm of damped SHO motion provides an excellent kinematic framework for characterizing the physiology of annular motion.

Importance of mitral annular oscillations. As predicted based on kinematic modeling, the results indicate that the MAO^+ group has superior longitudinal as well as global DF, both invasively and noninvasively determined, compared with the MAO^- group.

The MAO^+ group exhibited both greater annular excursion (cm) and a greater peak annular motion velocity (cm/s). Longitudinal stiffness and relaxation/viscoelasticity, which may become elevated in certain pathologies, were lower in these subjects. Longitudinal stored elastic strain, force, and strain-energy were increased, suggesting the availability of more energy for myocardial recoil. Similarly, global DF was better in the MAO^+ group as evidenced by a greater E/A (E/A > 1 in the MAO^+ group and E/A < 1 in the MAO^- group) and a lower A. These results are in concordance with the results for longitudinal function, as E′/A′ was greater in subjects with annular oscillations. Global relaxation, both before and during early filling, was clearly superior in the MAO^+ group, since τ, IVRT, and c were each lower in this group. The peak atrioventricular pressure gradient index, kx_o, was lower in the MAO^+ group. This indicates that a relatively greater atrioventricular pressure gradient is required in MAO^- subjects to adequately fill the LV in the presence of reduced elastic strain energy and increased resistance to filling (relaxation/viscoelasticity). That is, in energetic terms, filling in the MAO^+ group is more efficient than in the MAO^- group because a lower peak gradient suffices to generate comparable E wave-derived filling volumes (VTI_E: $P = 0.47$ between groups). This fact is easily understood when viewed in light of the lower c and c' values (dissipative effects) found in the MAO^+ group.

The elevated τ, IVRT, c, and c' indicate that LV relaxation during both isovolumic relaxation and early filling is impaired in MAO^- subjects relative to MAO^+ subjects. Although most of the indexes determined in this study are load dependent, the fact that load, as assessed by LVEDP, did not differ between groups indicates that the observed concordance of conventional and kinematic parameters/indexes that differentiated between the groups did so based on differences in the underlying physiology rather than load. Additionally, we emphasize that absence of MAO is indicative of prolonged τ, but not of elevated LV filling pressures (i.e., LVEDP) per se. Therefore, absence of MAO is best viewed as a marker for DD related to impaired LV relaxation.

Because the presence or absence of MAO is determined by whether c'^2 is less than or greater than $4k'$ (i.e., the sign of the parameter β'), there is no absolute cutoff for c' or k' for determination of MAO^+ or MAO^-. However, we note that lack of an absolute cutoff value does not limit clinical utility of annular "ringing." Given the reasonable sensitivity and specificity of MAO^- for identifying abnormal relaxation-related DF, noting the mere presence or absence of MAO may prove useful as an additive indicator in characterizing relaxation-related DD, particularly since the presence of MAO depends highly on LV (global and longitudinal) relaxation. Indeed, as pointed out by Aurigemma et al. (3), diagnosis of DD and diastolic heart failure requires the examination of multiple Doppler-echo parameters/indexes in concert since standard noninvasive DF indexes do not correlate well with invasive pressure-derived indexes. We stress that there is no need for off-line analysis of annular motion contours to utilize the information conveyed by MAO; all that is required is determining the presence or absence of MAO by visual inspection of the DTI image.

Limitations. Sample volume positioning during DTI may affect the shape of the DTI contour and thus longitudinal PDF parameters and indexes. However, the generous sample size

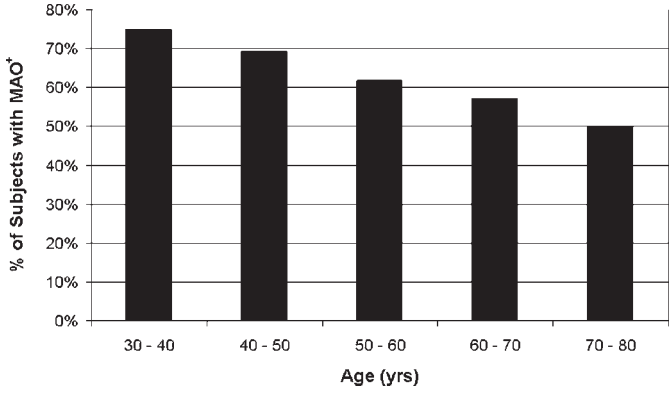

Fig. 3. Percentage of subjects with MAO as a function of age expressed per decade of age encompassing the full range of subject ages. Note that the percentage of subjects with MAO (MAO^+) decreases monotonically with age. This is concordant with the established progressive impairment of diastolic function associated with aging.

should minimize positioning-imposed effects. Neither the position nor size of the imaging sample length should affect the existence of MAO.

Only DTI of the lateral annulus was obtained, rather than other aspects, because, in general, it is echocardiographically easier to localize the sample volume at the lateral aspect and thereby minimize the likelihood of including tissue (myocardial) velocities. Several other studies have found that the motion of the septal and other aspects of the mitral annulus differs from the motion of the lateral annulus. Investigators have reported that the peak velocity of septal E′ waves is generally lower than that of lateral E′ waves and that the total annular excursion during early filling is lower for the septal aspect (1, 19). Based on prior observations, septal E′ and E″ are generally of lower amplitude than their lateral counterparts, and E″ is sometimes not observed even though oscillations of the lateral annulus may be seen in the same subject. We note that our modeling approach (the model, equations, methodology of computing parameters, etc.) does not depend on which aspect of the annulus is imaged.

While τ was significantly increased in the MAO^- group compared with the MAO^+ group, LVEDP was similar between groups. This finding may be at least partially explained by the fact that MAO occur during early filling (near E-wave termination), which is governed in part by the rate of LV relaxation, whereas LVEDP occurs at the end of late atrial filling (end of Doppler A-wave) and thus is influenced by atrioventricular interactions. Moreover, MAO occur during the pressure rise from LVP_{min} to LVP_{diast}, and the pressure difference from minimum to diastatic pressure ($LVP_{diast} - LVP_{min}$) differentiated between the MAO^+ and MAO^- groups better than LVEDP. The greater $LVP_{diast} - LVP_{min}$ in the MAO^+ group is evidence of enhanced suction-initiated filling in this group compared with the MAO^- group. This is further corroborated by the nearly significantly lower LVESV in the MAO^+ group and the additional concordant findings enumerated above.

The slightly increased HR in the MAO^- group may be thought to contribute to the longitudinal and global parameters/indexes that differentiated between groups. However, increased HR is primarily accommodated by a decrease in the duration of diastasis (7). E- and A-wave durations are nearly HR independent, as each decreases by <20% for a 100% increase in HR (6). DT has also been shown to decrease <20% for a 100% increase in HR and E to increase <12% (7). In light of the fact that DT was increased ($P = 0.11$) and peak E was decreased ($P = 0.34$) in the MAO^- group having the increased HR, other factors must be contributing to the decreased E/A in the MAO^- group. It is also notable that IVRT and τ, which would be expected to decrease with increasing HR, were actually increased significantly in the MAO^- group. The results indicate that increased (longitudinal and global) relaxation/viscoelasticity rather than increased HR in the MAO^- group is primarily responsible for the trends observed in these indexes.

Both groups included subjects with various nonvalvular comorbidities, notably hypertension, diabetes, and CAD. Because hypertension and diabetes are detrimental to DF and would be expected to correlate with the absence of MAO, their predominance in the subjects with oscillations suggests that exclusion of subjects with these comorbidities from the analysis would not alter the main findings. To verify this, we investigated the extent to which the inclusion of subjects with documented CAD and wall motion abnormalities on ventriculography influenced our results. Additionally, since LVEDP > 18 mmHg is often characteristic of DD, we investigated the influence of elevated LVEDP. Therefore, we divided both the MAO^+ and MAO^- groups into three subgroups and conducted subanalyses comparing the various global and longitudinal parameters and indexes between a given MAO^+ subgroup and its corresponding MAO^- subgroup. The subgroups were *1*) absence of wall motion abnormalities on ventriculography ($n = 45$), *2*) no history of CAD (i.e., <50% luminal narrowing on angiography) ($n = 41$), and *3*) LVEDP $\leq$ 18 mmHg ($n = 35$). While several supportive parameters/indexes lost significance, it is noteworthy that IVRT, c', k', and c remained significant in each subgroup, demonstrating that longitudinal stiffness and longitudinal and global relaxation during both early filling and isovolumic relaxation are important correlates of the absence of annular oscillations. In particular, it is noteworthy that these kinematic stiffness and relaxation/viscoelasticity indexes remained significant in the subgroup with LVEDP $\leq$ 18 mmHg. This finding implies that these indexes are capable of detecting relaxation-related DD before overt clinical manifestation based on invasively determined filling pressures. We note that the conventional Doppler indexes E′ and A remained significant in each subgroup as well. To determine whether a modified control group with normal LVEDP and normal τ would have a higher prevalence of MAO, we selected all subjects included in the study with LVEDP $\leq$ 18 mmHg and $\tau < 50$ ms without history of CAD or wall motion abnormalities. Of the 13 subjects that met these inclusion criteria, 10 (77%) had MAO.

Although MAO^+ and MAO^- likely depend on loading conditions in the LV, the load dependence of MAO could not be specifically determined in this study because of the similar LVEDP across groups. Future work is planned to address this issue.

Conclusions. The existence of oscillations of the mitral annulus during early filling is predicted by a unifying physical law that governs annular motion during early filling and whose parameters convey quantitative information regarding longitudinal (and global) diastolic function. Absence of oscillations implies elevated viscoelastic (i.e., impaired relaxation) effects relative to stiffness effects and reduced longitudinal stored strain energy to power early filling. The findings collectively indicate that absence of mitral annular oscillations is a marker of relaxation-related diastolic dysfunction. Importantly, absence of annular oscillations is not the cause, but rather is the consequence, of impaired diastolic function. These findings underscore the utility of considering the presence or absence of annular oscillation in concert with more commonly used noninvasive DF indexes, thereby providing insight into physiological mechanisms of dysfunction and facilitating identification of dysfunction in its preclinical state.

ACKNOWLEDGMENTS

We acknowledge sonographer Peggy A. Brown (Registered Cardiac Diagnostic Sonographer) for expert echocardiographic data acquisition.

GRANTS

This research was supported in part by the Whitaker Foundation (Roslyn, VA), the National Heart, Lung, and Blood Institute (Grants HL-54179 and

HL-04023 to S. J. Kovács), the Alan A. and Edith L. Wolff Charitable Trust (St. Louis, MO), and the Barnes-Jewish Hospital Foundation.

REFERENCES

1. **Alam M, Wardell J, Andersson E, Samad BA, Nordlander R.** Characteristics of mitral and tricuspid annular velocities determined by pulsed wave Doppler tissue imaging in healthy subjects. *J Am Soc Echocardiogr* 12: 618–628, 1999.
2. **Appleton CP, Firstenberg MS, Garcia MJ, Thomas JD.** The echo-Doppler evaluation of left ventricular diastolic function: a current perspective. In: *Cardiology Clinics*, edited by Crawford MH, Kovács SJ. Philadelphia, PA: Saunders, 2000, p. 513–546.
3. **Aurigemma GP, Zile MR, Gaasch WH.** Lack of relationship between Doppler indices of diastolic function and left ventricular pressure transients in patients with definite diastolic heart failure. *Am Heart J* 148: E12, 2004.
4. **Bauman L, Chung CS, Karamanoglu M, Kovács SJ.** The peak atrioventricular pressure gradient to transmitral flow relation: kinematic model prediction with in vivo validation. *J Am Soc Echocardiogr* 17: 839–844, 2004.
5. **Bland JM, Altman DG.** Measurement error proportional to the mean. *BMJ* 313: 106, 1996.
6. **Chung CS, Karamanoglu M, Kovács SJ.** The duration of diastole and its phases as a function of heart rate during supine bicycle exercise. *Am J Physiol Heart Circ Physiol* 287: H2003–H2008, 2004.
7. **Chung CS, Kovács SJ.** Consequences of increasing heart rate on deceleration time, the velocity-time integral, and E/A. *Am J Cardiol* 97: 130–136, 2006.
8. **Chung CS, Ajo DM, Kovács SJ.** Isovolumic pressure-to-early rapid filling decay rate relation: model-based derivation and validation via simultaneous catheterization echocardiography. *J Appl Physiol* 100: 528–534, 2006.
9. **Dent CL, Bowman AW, Scott MJ, Allen JS, Lisauskas JB, Janif M, Wickline SA, Kovács SJ.** Echocardiographic characterization of fundamental mechanisms of abnormal diastolic filling in diabetic rats with a parameterized diastolic filling formalism. *J Am Soc Echocardiogr* 14: 1166–1172, 2001.
10. **Duncan AM, Lim E, Gibson DG, Henein MY.** Effect of dobutamine stress on left ventricular filling in ischemic dilated cardiomyopathy. *J Am Coll Cardiol* 46: 488–496, 2005.
11. **Eucker SA, Lisauskas JB, Singh J, Kovács SJ.** Phase plane analysis of left ventricular hemodynamics. *J Appl Physiol* 90: 2238–2244, 2001.
12. **European Study Group on Diastolic Heart Failure.** How to diagnose diastolic heart failure. *Eur Heart J* 19: 990–1003, 1998.
13. **Firstenberg MS, Greenberg NL, Main ML, Drinko JK, Odabashian JA, Thomas JD, Garcia MJ.** Determinants of diastolic myocardial tissue Doppler velocities: influences of relaxation and preload. *J Appl Physiol* 90: 299–307, 2001.
14. **Garcia MJ, Rodriguez L, Ares M, Griffin BP, Thomas JD, Klein AL.** Differentiation of constrictive pericarditis from restrictive cardiomyopathy: assessment of left ventricular diastolic velocities in longitudinal axis by Doppler tissue imaging. *J Am Coll Cardiol* 27: 108–114, 1996.
15. **Gottdiener JS, Bednarz J, Devereux R, Gardin J, Klein A, Manning WJ, Morehead A, Kitzman D, Oh J, Quinones M, Schiller NB, Stein JH, Weissman NJ.** American Society of Echocardiography recommendations for use of echocardiography in clinical trials. *J Am Soc Echocardiogr* 17: 1086–1119, 2004.
16. **Hall AF, Kovács SJ.** Automated method for characterization of diastolic transmitral Doppler velocity contours: early rapid filling. *Ultrasound Med Biol* 20: 107–116, 1994.
17. **Hall AF, Bettlach JA, Nudelman SP, Kovács SJ.** Manufacturer and machine setting-based variation of parameters resulting from model-based image processing of echocardiographic transmitral Doppler velocity profiles. *Proceedings of the 1996 IEEE Ultrasonics Symposium*, 1996, p. 1205–1210.
18. **Hanley JA, McNeil BJ.** The meaning and use of the area under the Receiver Operating Characteristic (ROC) curve. *Radiology* 143: 29–36, 1982.
19. **Isaaz K, del Romeral LM, Lee E, Schiller NB.** Quantitation of the motion of the cardiac base in normal subjects by Doppler echocardiography. *J Am Soc Echocardiogr* 6: 166–176, 1993.
20. **Keren G, Sherez J, Megidish R, Levitt B, Laniado S.** Pulmonary venous flow pattern—its relationship to cardiac base dynamics. A pulsed Doppler echocardiographic study. *Circulation* 71: 1105–1112, 1985.
21. **Kovács SJ Jr, Barzilai B, Perez JE.** Evaluation of diastolic function with Doppler echocardiography: the PDF formalism. *Am J Physiol Heart Circ Physiol* 252: H178–H187, 1987.
22. **Kovács SJ, Rosado J, Manson McGuire AL, Hall AF.** Can transmitral Doppler E-waves differentiate hypertensive hearts from normal? *Hypertension* 30: 788–795, 1997.
23. **Kovács SJ, Meisner JS, Yellin EL.** Modeling of diastole. In: *Cardiology Clinics*, edited by Crawford MH, Kovács SJ. Philadelphia, PA: Saunders, 2000, p. 459–487.
24. **Kovács SJ, McQueen DM, Peskin CS.** Modelling cardiac fluid dynamics and diastolic function. *Phil Trans R Soc Lond* 359: 1299–1314, 2001.
25. **Lipton P.** Testing hypotheses: prediction and prejudice. *Science* 307: 219–221, 2005.
26. **Lisauskas JB, Singh J, Courtois M, Kovács SJ.** The relation of the peak Doppler E-wave to peak mitral annulus velocity ratio to diastolic function. *Ultrasound Med Biol* 27: 499–507, 2001.
27. **Lisauskas JB, Singh J, Bowman AW, Kovács SJ.** Chamber properties from transmitral flow: prediction of average and passive left ventricular diastolic stiffness. *J Appl Physiol* 91: 154–162, 2001.
28. **Lyseggen E, Rabben SI, Skulstad H, Urheim S, Risoe C, Smiseth OA.** Myocardial acceleration during isovolumic contraction: relationship to contractility. *Circulation* 111: 1362–1369, 2005.
29. **Nagueh SF, Middleton KJ, Kopelen HA, Zoghbi WA, Quiñones MA.** Doppler tissue imaging: a noninvasive technique for evaluation of left ventricular relaxation and estimation of filling pressures. *J Am Coll Cardiol* 30: 1527–1533, 1997.
30. **Nagueh SF, Lakkis NM, Middleton KJ, Spencer WH, Zoghbi WA, Quiñones MA.** Doppler estimation of left ventricular filling pressures in patients with hypertrophic cardiomyopathy. *Circulation* 99: 254–261, 1999.
31. **Naqvi TZ.** Diastolic function assessment incorporating new techniques in Doppler echocardiography. *Rev Cardiovasc Med* 4: 481–499, 2003.
32. **Nikitin NP, Witte KK, Thackray SD, de Silva R, Clark AL, Cleland JG.** Longitudinal ventricular function: normal values of atrioventricular annular and myocardial velocities measured with quantitative two-dimensional color Doppler tissue imaging. *J Am Soc Echocardiogr* 16: 906–921, 2003.
33. **Nikitin NP, Witte KK, Ingle L, Clark AL, Farnsworth TA, Cleland JG.** Longitudinal myocardial dysfunction in healthy older subjects as a manifestation of cardiac ageing. *Age Ageing* 34: 343–349, 2005.
34. **Nishimura RA, Jaber W.** Understanding "diastolic heart failure." *J Am Coll Cardiol* 49: 695–697, 2007.
35. **Persson H, Lonn E, Edner M, Baruch L, Lang CC, Morton JJ, Östergren J, McKelvie RS.** Diastolic dysfunction in heart failure with preserved systolic function: need for objective evidence. *J Am Coll Cardiol* 49: 687–694, 2007.
36. **Popovic ZB, Prasad A, Garcia MJ, Arbab-Zadeh A, Borowski A, Dijk E, Greenberg NL, Levine BD, Thomas JD.** Relationship among diastolic intraventricular pressure gradients, relaxation, and preload: impact of age and fitness. *Am J Physiol Heart Circ Physiol* 290: H1454–H1459, 2006.
37. **Riordan MM, Chung CS, Kovács SJ.** How diabetes affects diastolic function: determination of stiffness and relaxation from transmitral flow. *Ultrasound Med Biol* 31: 1589–1596, 2005.
38. **Riordan MM, Kovács SJ.** Quantitation of mitral annular oscillations and longitudinal "ringing" of the left ventricle: a new window into longitudinal diastolic function. *J Appl Physiol* 100: 112–119, 2006.
39. **Sohn DW, Chai IH, Lee DJ, Kim HC, Kim HS, Oh BH, Lee MM, Park YB, Choi YS, Seo JD, Lee YW.** Assessment of mitral annulus velocity by Doppler tissue imaging in the evaluation of left ventricular diastolic function. *J Am Coll Cardiol* 30: 474–480, 1997.
40. **Tsakiris AG, Von Berath G, Rastelli GC, Bourgeois MJ, Titus JL, Wood EH.** Size and motion of the mitral valve annulus in anesthetized intact dogs. *J Appl Physiol* 30: 611–618, 1971.
41. **Wiggers CJ.** Dynamics of ventricular contraction under abnormal conditions. *Circulation* 5: 321–348, 1952.
42. **Zaky A, Grabhorn L, Feigenbaum H.** Movement of the mitral ring: a study in ultrasonography. *Cardiovasc Res* 1: 121–131, 1967.